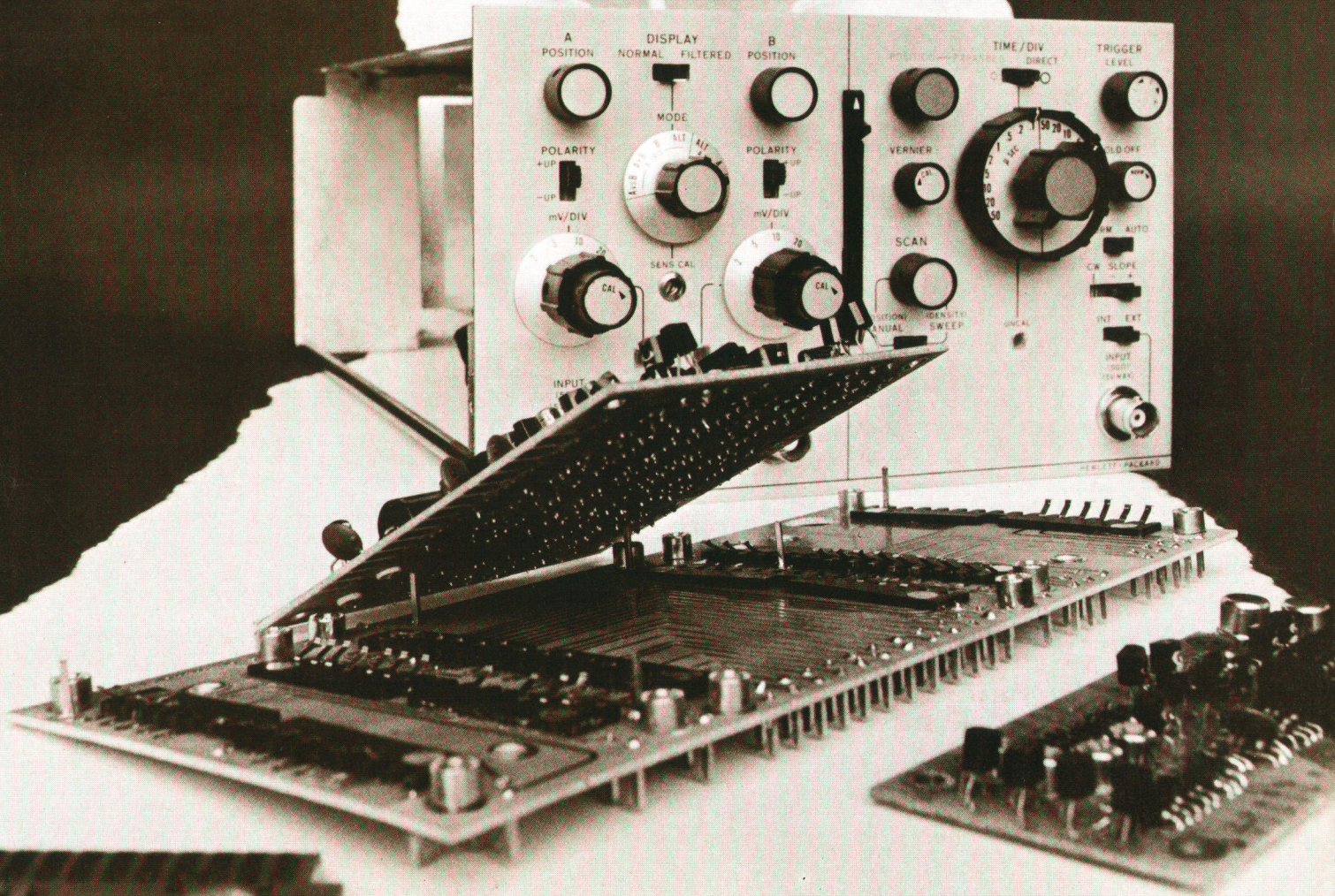
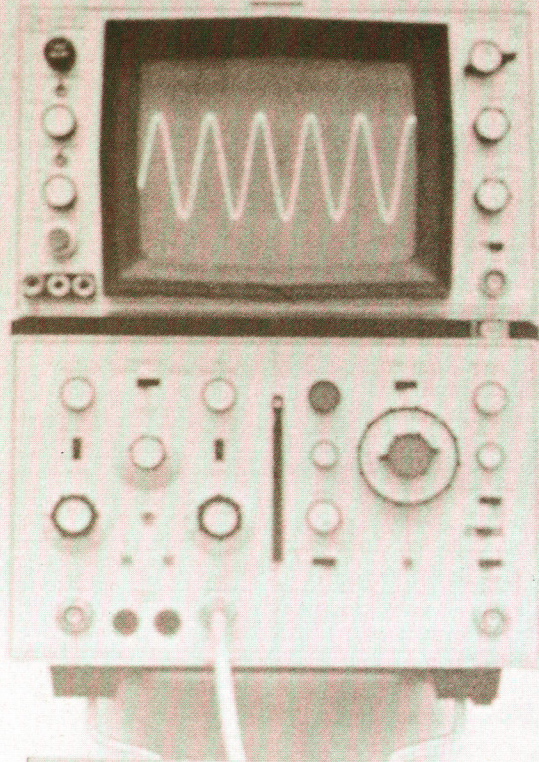


NOVEMBER 1971

# HEWLETT-PACKARD JOURNAL



# A Scrutable Sampling Oscilloscope

*Some find sampling scopes enigmatic, choosing to forego their high-frequency response and sensitivity rather than use them. Here's a sampling scope for people who don't like sampling scopes. New circuit ideas make it as easy to use as a real-time scope.*

**By William Farnbach**

DESPITE RECENT ADVANCES in the performance of real-time oscilloscopes, sampling techniques still have the edge when viewing signals with very fast transitions or very high frequency components. The sensitivity and extended high-frequency response of sampling instruments are just what's needed for studying fast waveforms in high-speed digital circuits (Fig. 1).

In addition to fast, sensitive response, sampling oscilloscopes have other singular characteristics. Only sampling scopes have high-frequency response on the Y axis as well as the X axis, and are thus the only means of viewing X-Y plots of high-frequency signals (Fig. 2). Another of their special characteristics is immunity to amplifier overload. Sampling scopes can magnify waveforms enormously for studying fine detail without loss of fidelity—the deflection amplifiers easily recover from an overload condition between successive sampling pulses.

And now, with a new 1-GHz dual-channel sampling scope plug-in to be described here, sampling scopes become the most economical means of viewing high-frequency signals. Sampling scopes now cost less than any real-time scope capable of response above 100 MHz.

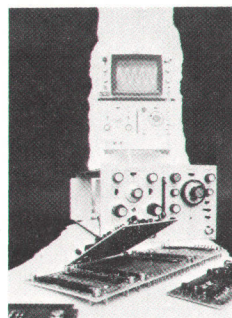
The trade-off is that sampling scopes require repetitive signals—they cannot display the whole of a waveform that occurs only once, the way real-time scopes can.

## Historical roots

Sampling techniques were used over 100 years ago to translate alternator waveforms to a time scale that could be accommodated by available instruments. And about 20 years ago, the same concept was applied to oscilloscopes to view waveforms of several hundred MHz on low-frequency

cathode-ray tubes.<sup>1</sup>

Sampling oscillography really came of age 12 years ago with the introduction of the HP Model 185A.<sup>2</sup> By use of a closed-loop feedback sampling system—a technique now used in all sampling scopes—this oscilloscope achieved the needed amplitude stability that the earlier open-loop sampling systems lacked. In addition, the two-channel display and high-impedance probes of this instrument made it a truly general-purpose instrument. With this instrument, sampling oscillography quickly became established as the way to study high-speed waveforms.



**Cover:** *Simplicity of design and operation is implied by HP Journal Art Director Arvid Danielson's photo of parts of the new Model 1810A Sampling Oscilloscope plug-in. Designed for those who would rather not hold the instruction manual in one hand while twiddling knobs with the other, the new Sampling Scope is as*

*straightforward and tractable as a real-time scope.*

## In this issue:

*A Scrutable Sampling Oscilloscope,*  
by William Farnbach ..... **page 2**

*Frequency Stability Measurements*  
by Computing Counter System,  
by David Martin ..... **page 9**

*More Informative Impedance*  
*Measurements, Swept from 0.5*  
*to 110MHz, by Julius K. Botka* ..... **page 15**

*Time Step and Elimination of the*  
*Frequency Offset of the UTC System* ..... **page 20**

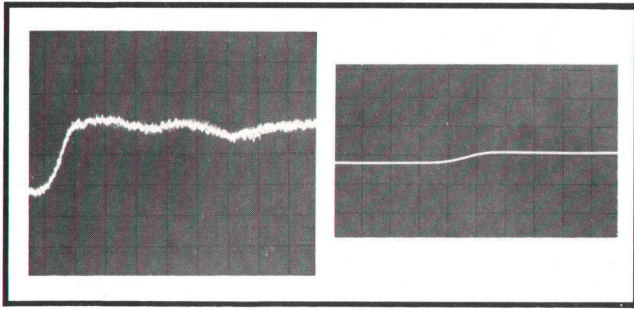


**Fig. 1.** Oscillograms contrast performance of sampling scope with that of real-time scope, one that has performance most closely approaching sampling scope at time of writing. Photo at left shows low-amplitude, fast-risetime pulse (4mV, 30ps  $t_r$ ) displayed by new Model 1810A 1GHz sampling plug-in in 180A mainframe (deflection factor is 2 mV/div, sweep speed is 500ps/div). Photo at right shows same pulse on 183A/1830A/1840A 250MHz real-time scope (deflection factor: 10mV/div, sweep speed: 1ns/div).

### Adolescent growth

The 500-MHz performance of the original Model 185A was made possible by fast-switching diodes developed in Hewlett-Packard's own solid-state laboratories. Newer diodes, and exploitation of the step-recovery principle, soon raised performance to 1 GHz. Then, new sampler circuits made 4 GHz possible, and ultimately a sampler was developed that achieved frequency response of 12.4 GHz.<sup>3</sup> This has now been extended to 18 GHz.

Nevertheless, not everyone who could use a sampling scope's special characteristics would use them willingly. Some were perplexed by a sampling scope's esoteric controls. Others balked at price, preferring to live within the limitations of conventional real-time scopes.

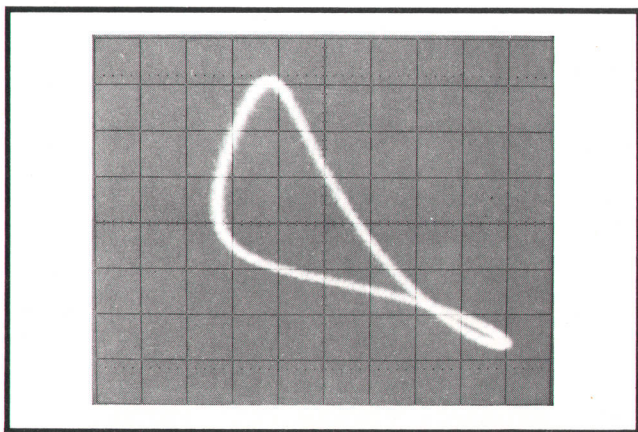


**Fig. 2.** Sampling scope can display higher frequency X-Y plots than any real-time scope, as shown by this Lissajous pattern made by distorted sine wave with 500MHz fundamental frequency.

### Signs of maturity

Thus ease of operation, low price, and serviceability, rather than increased bandwidth or sensitivity, became the design goals for the newest HP 1-GHz sampling scope, the Model 1810A plug-in for the HP 180-series oscilloscopes. This shift in objectives indicates that sampling oscillography is reaching a state of maturity.

Success of the effort may be judged by Fig. 3. On the new sampling scope, the  $T_R$  CAL and SMOOTHING controls have been eliminated, and the SCAN control has been simplified by eliminating seldom-used functions. The TRIGGER controls look—and behave—very much like those of a real-time scope. The photo shows how much like familiar real-time plug-ins the new sampling plug-in is.

The price is several hundred dollars less than previous 1-GHz sampling scopes, and lower than any 100-MHz real-time scope. Part of this lower cost is a consequence of advancing technology—inexpensive monolithic operational amplifiers and logic modules cut the cost of those parts of the circuitry where they can be used. HP's own component developments contributed too—a printed-circuit switch designed for other instruments is used for the time-scale switch, reducing the number of wafers from 12 to 2. Not only does this switch reduce labor costs, but the savings in space alleviates the need for expensive miniature components elsewhere in the plug-in.

A good part of the cost reduction resulted from an intense examination of each circuit function in an effort to find better ways of accomplishing the same job at lower cost. Examples will be described later here.

Serviceability, although a design goal in all HP instruments, was given such high priority with this instrument that it called for redesign of several circuits just to get rid of adjustments. As a result, the number of internal adjustments has been cut from the usual 45 or 50 to just 15, and these are non-interacting. Set up and calibration are thus far easier, not only reducing production costs but also shortening turnaround time in the service shop.

Assembly and disassembly are fast, too. The circuit boards are mounted parallel with the motherboard, to shorten signal paths, and board-to-board contact is made through spring clips (Fig. 4). Board removal requires only removal of four screws and, in those few cases where a lead must be detached, only one wire needs unsoldering.

The printed-circuit time base switch brings another advantage here—it can be removed by un-

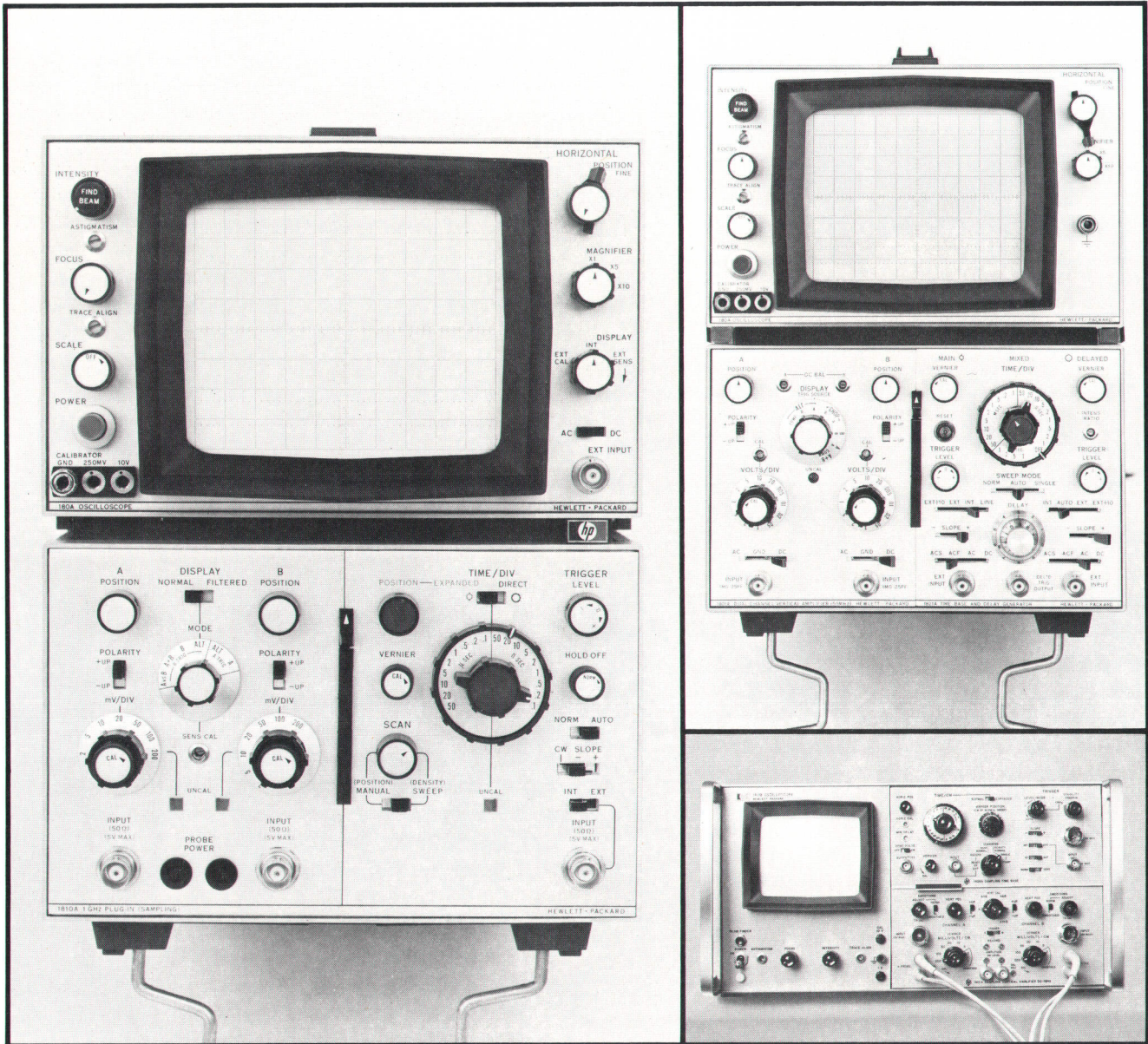


Fig. 3. Front panel of new Model 1810A Sampling plug-in (top left) is no more complicated than conventional real-time scope (top right). Several controls required by previous generation sampling scopes (bottom) have been eliminated.

plugging one connector, taking off the knobs, and undoing one nut and one screw. This used to be one of the most difficult and time-consuming service operations in a sampling scope.

### Going full-circle

It is interesting to note that whereas the development of a high-impedance sampling probe was one of the features that made the original Model 185A Sampling Oscilloscope so readily accepted,

the new Model 1810A plug-in uses 50Ω inputs. This is because hybrid and monolithic integrated circuit technology has pretty well standardized on a circuit impedance of 50 ohms, and the smoothness of a 50Ω input now becomes more important than high impedance. Earlier sampling scopes achieved not much better than 15% reflections from 50Ω input arrangements but the new 1810A inputs reflect less than 6% of the signal.

Where high input impedance may still be preferred, a Model 1120A Active Probe is easily

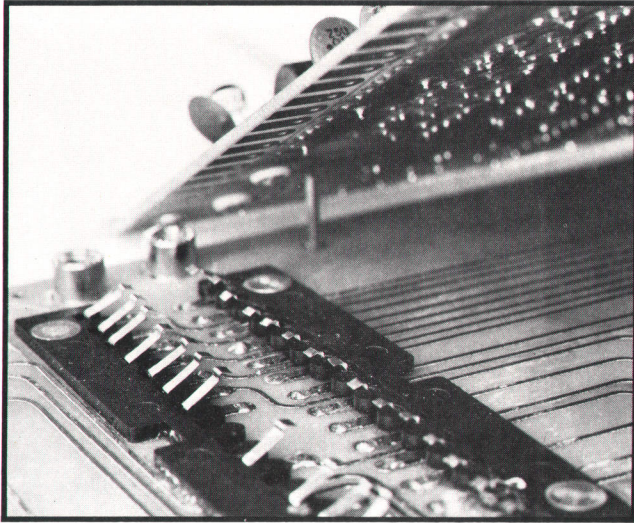


**Fig. 4.** Gold-plated metal fingers make board-to-board electrical contact, eliminating cabling, speeding assembly.

attached to this instrument to give  $100\text{k}\Omega$  impedance (shunted by  $2\text{ pF}$ ). The upper frequency limit is then  $500\text{ MHz}$ , the same as the original Model 185A, but unlike the earlier scopes, this arrangement has the advantage of obtaining high-impedance while the delay line is still in the signal path, allowing internal triggering.

#### Inexpensive quality

Now for a look at how all this was accomplished. The delay lines are a good example. It once was necessary to use expensive precision  $50\Omega$  coaxial cable for the signal delay lines to assure waveform fidelity. Now, high-frequency losses aren't so much of a problem because the delay can be shorter as a result of other developments that reduced the dead time between trigger and strobe. This means that less expensive cable can be used.

The new delay-line circuit is shown in Fig. 5. It uses inexpensive  $75\Omega$  cable terminated in a broadband constant-R network rather than an inductively compensated resistor. By careful choice of the trigger pick-off resistor, an excellent  $50\Omega$  impedance match at the input is achieved. The cost is one-tenth that of the older system at a small sacrifice in minimum deflection factor ( $2\text{ mV/div}$  instead of  $1\text{ mV/div}$ ).

Reflections from this input are now determined by the 'cleanness' of circuit layout rather than by the amount of degradation in trigger sensitivity that can be tolerated. Formerly, the trigger pick-off at the delay line input was designed to draw as little power as possible from the signal to mini-

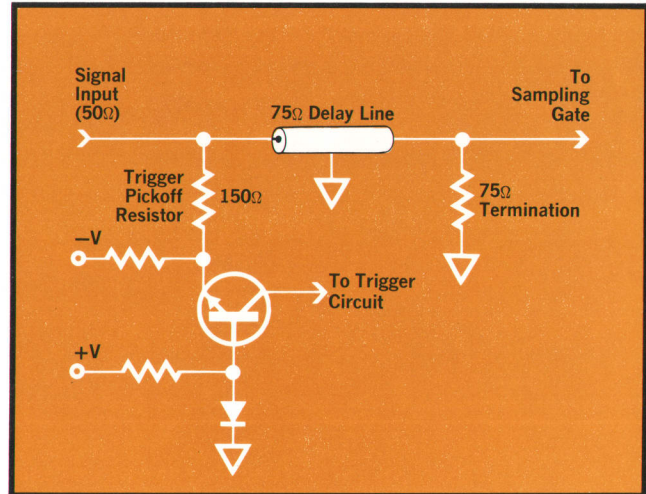


**Fig. 5.** New input circuit makes one-third of input power available for triggering while eliminating need for precision impedance delay line.

mize the input impedance mismatch. With the new circuit, one-third of the input signal can be withdrawn for triggering while still maintaining an excellent impedance match.

By making available greater trigger power, the new input arrangement substantially improves the triggering characteristics of the plug-in—sweeps trigger reliably with less than  $0.03\text{ ns}$  jitter on  $100\text{ mV}$  signals, and useful triggering can be obtained with  $5\text{ mV}$  signals.

Triggering characteristics were also improved as a result of insights provided by a computer model, based on an analysis of multiple triggering.<sup>4</sup> The computer model disclosed that the optimum relationship between the trigger level control and trigger sensitivity (the MODE control on earlier scopes) is independent of the shape of the triggering signal. As a result of this disclosure, the LEVEL and MODE functions were combined into one TRIGGER LEVEL control circuit. Not only does this achieve one-knob trigger control, but it eliminates the possibility of unsuitable LEVEL/MODE combinations, a potential source of frustration with two-knob control.

#### Bettering the improved

As in other HP 1-GHz sampling scopes, the new Model 1810A uses a four-diode sampling gate, shown in Fig. 6. To take a sample, the balanced strobe pulse turns on the diodes briefly, about  $350\text{ ps}$ , transferring a charge to the sampling capacitor, a charge that is proportional to the difference between the input and sampling capacitor voltages.

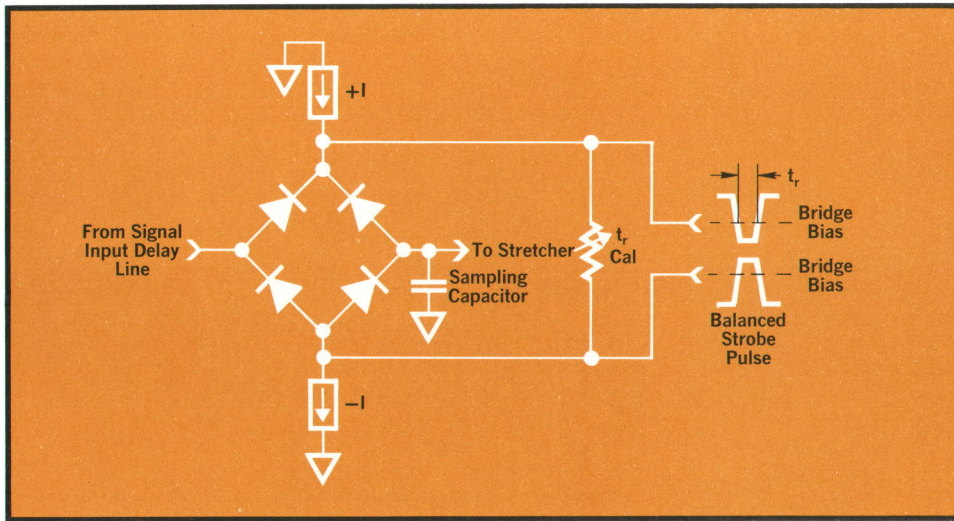


**Fig. 6.** Sampling gate in new plug-in. Amplitude of squared-off strobe (sampling) pulse affects system risetime much less than amplitude of triangular strobe pulse of earlier instruments.

It used to be that the amplitude of the triangular strobe pulse was very sensitive to temperature, causing changes in the width of the strobe pulse at the turn-on level which in turn affects system risetime. The  $T_R$  CAL control adjusted the diode bias to correct for these changes.

Now, with newer transistors and diodes, and by meticulous attention to design and layout, the new strobe generator puts out a larger strobe pulse with steeper sides and a truncated top. It is far less susceptible to temperature, and any amplitude changes that do occur have less effect on the gate-open time. Hence, the  $T_R$  CAL adjustment no longer needs to be on the front panel.

#### Switching out the switch

Following the sampler, a stretcher circuit amplifies the sample pulse up to the actual value of the waveform at the instant of sampling, and it retains the value for use by the display circuits. It also feeds the new value back to the sampling capacitor to complete its charge.

Once upon a time the stretcher included a switch that turned on just long enough to bring the stretcher capacitor up to the new value. This switch required a fairly high-level signal to achieve linearity, so the circuit also had an attenuator to accommodate a wide range of input voltages. Consequently, a corresponding attenuator was needed in the feedback path. Getting the two attenuators to track required a number of adjustments. A SMOOTHING control, which adjusted internal amplifier gain, was included to compensate for any mistracking.

Now there is a new stretcher circuit, shown in Fig. 7. This one has no switch. Instead, it uses

a differential amplifier with a 'balance' capacitor at one input. Following the sampling instant, the sample capacitor dumps some of its new charge into the balance capacitor. The output of the differential amplifier is therefore a pulse that drops back to the zero level within a microsecond or so as the voltages on the sampling and balance capacitors equalize.

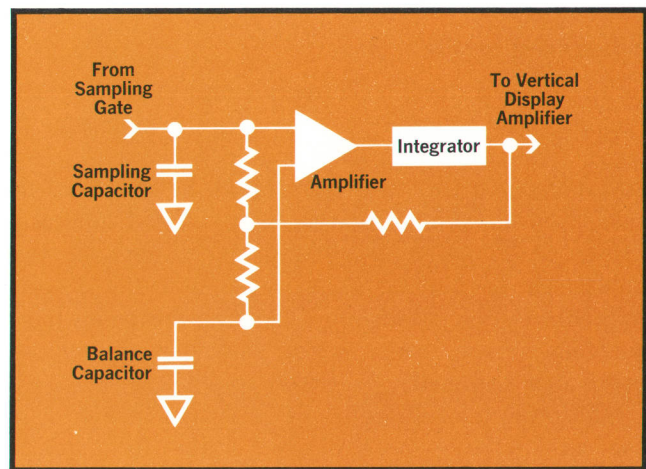


**Fig. 7.** Stretcher circuit processes signal samples, retaining sample amplitude in integrator for display between sampling instants. New circuit eliminates tracking attenuators and several adjustments.

The integrator output moves to a new level in response to the pulse out of the differential amplifier, without use of a switch. A single attenuator can now be used at the output of the integrator so, with no attenuator in the feedback loop to track, there's no need for a SMOOTHING control on the front panel.

### Inexpensive simplicity

The trigger pick-off amplifier is a good example of how inexpensive IC's helped reach design goals. As in earlier instruments, the 1810A uses a common-base amplifier to get high-frequency response and a 'clean' input impedance. The base voltage must be offset, though, if there is to be no offset at the signal input.

Formerly, a compensating offset was provided by a diode that would roughly track any temperature-caused changes in the emitter. The bias on the diode was set initially by a potentiometer to bring the emitter offset to zero.

Now, an inexpensive IC operational amplifier, used in place of the potentiometer as shown in Fig. 8, automatically adjusts diode bias to maintain the input of the trigger input amplifier at ground potential—and an adjustment is eliminated. Besides, temperature-induced offsets at the input are reduced to less than 3mV over the operating range of the instrument (0 to +55°C).

### Deserving another good turn

A similar technique is used in the horizontal scan generator. This circuit steps the CRT beam horizontally with an integrator that charges up incrementally immediately following each sample.

In earlier instruments, the integrator was reset at the end of a sweep simply by shorting the integrating capacitor with an electronic switch. Since the integrator's feedback capacitor must retain its charge between samples, an FET is used as the input to the integrator but the FET and the electronic switch both contribute offsets. These offsets were compensated for with an internal 'staircase offset' adjustment and a front-panel 'MINIMUM OFFSET' control.

In the new circuit, an IC op amp with one input grounded is in series with the electronic reset switch (the scan generator output goes to the other input). During reset, inclusion of the op amp in the feedback loop clamps the scan generator output to ground. Regardless of the operating temperature, there is no more than 20mV variation in the clamped voltage.\* Thus, the staircase offset and MINIMUM DELAY adjustments are no longer needed.

\* Variations in the clamped voltage affect the length of signal delay needed to insure display of the first sample, as these variations affect the time required for the fast ramp—started by the trigger pulse—to reach coincidence with the clamped voltage (a sample is taken whenever the fast ramp coincides with the scan generator's staircase voltage).

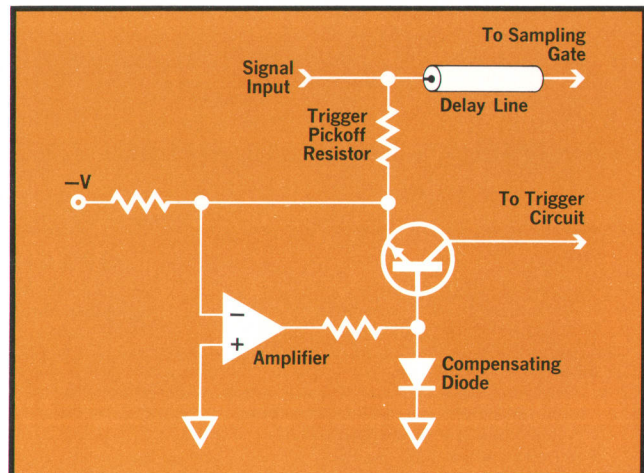
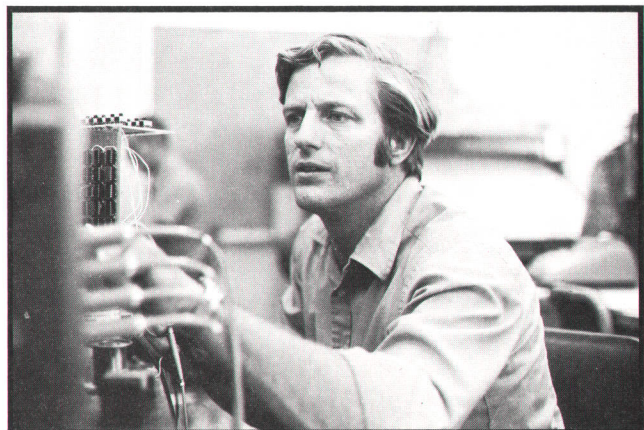


Fig. 8. Trigger pick-off circuit uses IC amplifier to eliminate input offset normally associated with common-base amplifiers.

### Acknowledgments

John Wagstaff and Jeffrey Smith contributed to the circuit design of the new sampling plug-in. Product design was by James Arnold, Robert Montoya, and George Blinn. The author would also like to thank Edward Prijatel for his contributions and the engineering support group for theirs. 🍷



### William Farnbach

Before assuming project leadership on the Model 1810A Sampling plug-in, Bill Farnbach worked on the 1424A and 1425A Sampling Time Bases for the 140-series Oscilloscope system, and the 1817A sampling head for the 1815A TDR/12.4GHz sampling plug-in for the 180-series Oscilloscope system.

Bill joined HP in 1967 upon getting his MSEE degree from Brigham Young University, where he also earned his BSEE degree.

## References,

1. J. G. McQueen, "The Monitoring of High-Speed Waveforms," *Electronic Engineering*, pp 436-441, Oct. '52.
2. R. Carlson et al, "Sampling Oscillography," 1959 IRE Wescon Convention Record, part 8, pp 44-51.

3. A. I. Best, D. L. Howard, and J. M. Umphrey, 'An Ultra-Wideband Oscilloscope Based on an Advanced Sampling Device,' *Hewlett-Packard Journal* Oct. 1966.
4. R. McMorrow and W. Farnbach, "A Novel Approach to High Frequency Trigger Circuit Design," 1969 Wescon Technical Papers, Session 13.

## SPECIFICATIONS HP Model 1810A Sampling Plug-in (for 180 System)

### MODES OF OPERATION

Channel A; channel B; channels A and B displayed on alternate samples (ALT); channel A plus channel B (algebraic addition); and channel A versus channel B.

### VERTICAL CHANNELS

BANDWIDTH: dc to 1 GHz.

RISE TIME: <350 ps.

PULSE RESPONSE: <3% (overshoot and perturbations).

DEFLECTION FACTOR:

Ranges: 2 mV/div to 200 mV/div in 1, 2, 5 sequence.

Accuracy:  $\pm 3\%$ .

Vernier: Provides continuous adjustment between ranges; extends minimum deflection factor to <1 mV/div.

Polarity: +UP or -UP.

DYNAMIC RANGE: >1.6 V.

POSITIONING RANGE:  $\geq \pm 1$  V on all deflection factors.

INPUT R:  $50\Omega$ ,  $\pm 2\%$ .

MAXIMUM INPUT:  $\pm 5$  V (dc + peak ac).

VSWR: <1.1:1 to 300 MHz, increasing to <1.5:1 at 1 GHz.

REFLECTION COEFFICIENT: <6%, measured with HP Model 1415A TDR.

NOISE:

Normal: <2 mV, observed from center 80% of dots.

Filtered: <1 mV.

ISOLATION BETWEEN CHANNELS:  $\geq 40$  dB with 350 ps risetime input.

TIME DIFFERENCE BETWEEN CHANNELS: <100 ps.

A + B OPERATION: Bandwidth and deflection factors unchanged; either channel may be inverted for  $\pm A \pm B$  operation.

VERTICAL OUTPUTS: Uncalibrated 1 V signal from each channel at rear panel of 180 system mainframes.

### TIME BASE

RANGES:

Normal: 10 ns/div to 50  $\mu$ s/div in 1, 2, 5 sequence.  $\pm 3\%$  accuracy with vernier in calibrated position.

Expanded: Direct reading expansion up to  $\times 100$  in seven calibrated steps on all normal time scales, extends range to 100 ps/div. Accuracy is  $\pm 4\%$  (10 ps/div,  $\pm 10\%$ , using mainframe magnifier).

VERNIER: Continuously variable between ranges; increases fastest sweep to <40 ps/div.

TRIGGERING MODE:

Normal: Trigger level control can be adjusted to trigger on wide variety of internal or external signals.

Automatic: Triggers automatically on most internal or external signals with minimum of adjustment of level control. Baseline displayed in absence of input signal.

External:

Sine Wave: 30 mV p-p for signals from 1 kHz to 1 GHz for jitter of <30 ps plus 1% of one period. Useful triggering can be obtained with 5 mV signals.

Pulse: 30 mV peak, 3 ns wide pulses for <30 ps jitter. Useful triggering can be obtained with 5 mV signals.

Internal:

Source: Selectable; on channel A for channel A alone or alternate; on channel B for channel B alone, alternate, A + B, or A vs B.

Sine Wave: 30 mV p-p for signals from 1 kHz to 200 MHz, 100 mV p-p for signals from 200 MHz to 1 GHz for jitter of <30 ps plus 1% of one period. Useful triggering can be obtained with 5 mV signals.

Pulse: Same as external.

Either internal or external:

Auto: 50 mV p-p for CW signals from 1 kHz to 200 MHz for <30 ps jitter plus 2% of one period (may be used to 1 GHz with increased jitter). Pulse triggering requires 50 mV peak, 3 ns wide pulses for <30 ps jitter.

Level and Slope: Continuously variable from +800 mV to -800 mV on either slope of sync signal.

Coupling: AC coupling attenuates signals below approx 1 kHz.

TRIGGER STABILITY: Holdoff variable over at least 3:1 range in all sweep modes.

MARKER POSITION: Intensified marker segment indicates point about which sweep is to be expanded.

SCAN:

Internal: Dot density continuously variable from 100 to 1000 dots full screen; from approx. 500 to 2000 dots in filtered mode.

Manual: Scan is positioned manually by front-panel control.

HORIZONTAL OUTPUT: Uncalibrated 0.75 V signal at rear panel of 180 or 181 mainframe.

### GENERAL

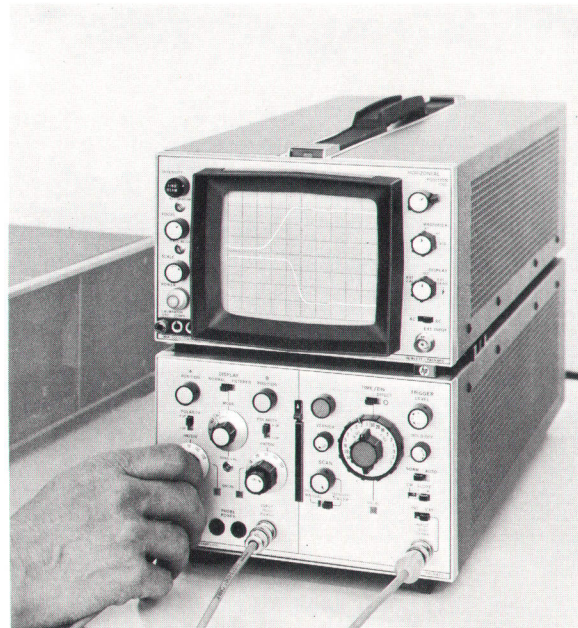
PROBE POWER: Supplies power to operate two HP active probes.

WEIGHT: Net, 7 lb (3.2 kg.); shipping, 12 lb (5.4 kg.).

ENVIRONMENT: (Plug-in operates within specifications over following ranges.) Temperature, 0°C to 55°C; Humidity, to 95% relative humidity to 40°C; Altitude, to 15,000 ft; Vibration, in three planes for 15 min. each with 0.010 inch excursion, 10 to 55 Hz.

PRICE: Model 1810A, \$1650.00

MANUFACTURING DIVISION: COLORADO SPRINGS DIVISION  
1900 Garden of the Gods Road  
Colorado Springs, Colorado 80907



# Frequency Stability Measurements by Computing Counter System

Here are methods for making either time-domain or frequency-domain measurements conveniently, accurately, and with high resolution.

By David Martin

OSCILLATORS are supposed to be sources of pure single-frequency sinusoidal waveforms. But then, nothing's perfect. The outputs of real-world frequency sources are contaminated by varying amounts of amplitude and frequency noise or instabilities.

In a time- or frequency-based system the information capacity may be largely determined by the stability of a reference oscillator or timing generator. For example, the range resolution of a radar depends on the stability of the local oscillator. Similarly, timing instabilities increase the error rate in a digital communication system.

Because frequency stability affects system performance so much, there is a continuing need for accurate measurements of it. A particularly convenient way to make such measurements is with the HP 5360A Computing Counter System. Besides being convenient, the system is highly accurate, and it can make noise measurements at extremely small frequency offsets (e.g., 0.01 Hz) from the nominal, center, or carrier frequency of the oscillator.

## Representations of Frequency Stability

The random perturbations which show up as instabilities in the frequency of an oscillator can be represented in either the frequency domain or the time domain. In the frequency domain the quantity most commonly used to describe these instabilities is the *single-sideband-to-carrier* (SSB/C) *phase-noise power ratio*. A typical graphic plot of this ratio is shown in Fig. 1. Such a plot shows the distribution of noise power as a function of frequency offset from the carrier. For example, Fig. 1 indicates that the noise power is 73 dB

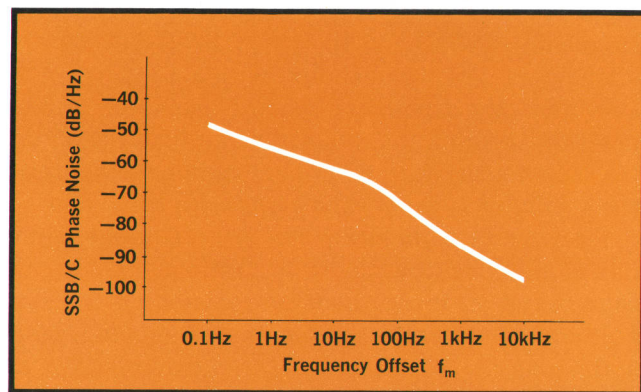


Fig. 1. Typical plot of single-sideband-to-carrier phase-noise power ratio of an oscillator as a function of offset from nominal or carrier frequency.

down from the carrier power in a 1 Hz bandwidth at an offset of 100 Hz from the carrier. Total noise power in any frequency band is obtained by integrating this curve. Integration of Fig. 1 between 0.1 Hz and 10 kHz yields a total noise power of -46 dB. If one assumes that the other sideband is the mirror image of the one shown, then the noise this sideband contributes is also -46 dB. Thus, the *total phase-noise power* of the signal, in a 20 kHz band centered about the carrier frequency but excluding the center 0.2 Hz, is 43 dB down from the carrier signal power.

In the time domain these same random perturbations are quantitatively defined by the *fractional frequency deviation* (also called *short term stability*) of the oscillator. A typical illustration of this time domain representation is shown in Fig. 2. An example of interpreting Fig. 2 is as follows. For a 1 ms averaging time  $\tau$ , the fractional frequency

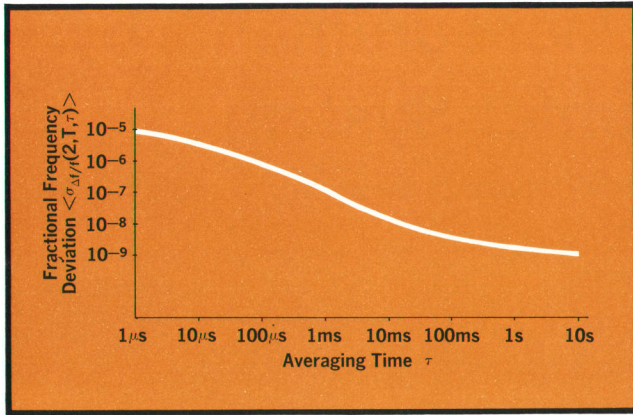


Fig. 2. Typical plot of fractional frequency deviation of an oscillator as a function of averaging time  $\tau$ .

deviation shown in Fig. 2 is  $1 \times 10^{-7}$ . If the nominal oscillator frequency is 1 MHz then the fractional frequency deviation in Hz is  $1 \times 10^6 \times 1 \times 10^{-7} = 0.1$  Hz rms. This implies that with a 1 ms observation time, the frequency of this oscillator can be determined to an uncertainty of no better than 0.1 Hz. This uncertainty is, of course, due to the noise the oscillator is generating along with the signal.

Figs. 1 and 2 illustrate the two different methods of representing the same phenomenon. Which representation is more useful depends on the system involved. For example, radar ranging measurements are basically measurements of time, so the time-domain or fractional-frequency-deviation measurement is the more meaningful. Conversely, noise power and bandwidth are prime considerations in communicating with deep-space probes,

so the frequency-domain representation would be used.

### The Computing Counter System

Whichever representation is decided upon, the computing counter system<sup>1,2,3</sup> can make the measurements easily, conveniently, and accurately.

The computing counter system can be compared to a general-purpose computer-instrument system in that it has the ability to perform measurements (for example frequency), and then to mathematically reduce the raw measured data to the desired form. The major element of the system is the HP 5360A Computing Counter, an instrument which in fact is a unique hybrid of high-speed measurement circuits and an arithmetic unit capable of performing the basic mathematical functions. With the 5365A Input Module the counter has a 320 MHz direct frequency measurement capability. Plug-ins extend this to 18 GHz. The counter can also measure the time between two events with the 5379A Time Interval Plug-in, and voltage with the 2212A Voltage-Frequency Converter.

The computing counter system is completed with either of two programming devices, the 5376A Programmer or the 5375A Keyboard. These devices give the user access to the arithmetic capability of the computing counter, in much the same way as a teleprinter provides access to a computer. By appropriately programming either of these devices the user can mathematically reduce the raw measured data to its final desired form. Fig. 3 is a photo of a computing-counter system.

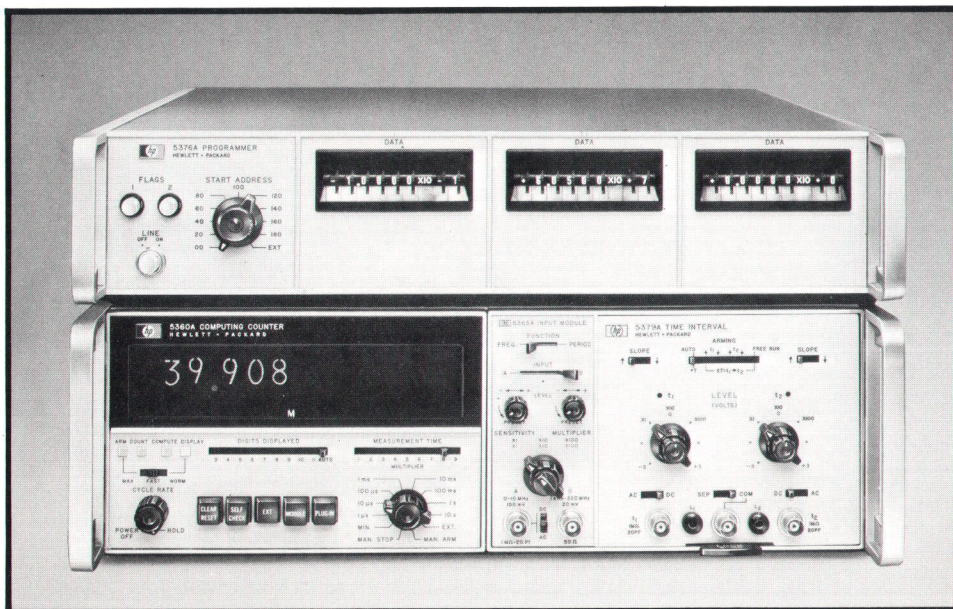


Fig. 3. Hewlett-Packard 5360A Computing Counter System makes frequency-stability measurements in either the time domain or the frequency domain. Shown here is the 5360A Computing Counter (lower unit) with the 320 MHz 5365A Input Module, the 5379A Time Interval Plug-in, and the 5376A Programmer (upper unit). In lieu of the 5376A, the 5375A Keyboard may be used as a programming device.

### Time-Domain Stability Measurements — Fractional Frequency Deviation

Fractional frequency deviation is the term used to describe the frequency instabilities of a source in the time domain. It has been shown<sup>4,5</sup> that a meaningful quantitative measure of fractional frequency deviation is given by the Allan variance:

$$\langle \sigma_{\Delta f/f}(2, T, \tau) \rangle = \frac{1}{f_0} \sqrt{\frac{1}{2N} \sum_{i=1}^N (f_i - f_{i-1})^2} \quad (1)$$

where  $f_i$ ,  $f_{i-1}$  are individual successive measurements of the oscillator frequency,  $N$  is the number of measurements made,  $f_0$  is the nominal mean frequency of the oscillator,  $T$  is the time between measurements, and  $\tau$  is the averaging (or measurement) time of each frequency measurement. This equation is derived from the classic formula for sample variance. It is statistical in nature, so for good confidence levels the number of samples  $N$  should be large (e.g.,  $N = 100$ ). The measurement is dependent on averaging time  $\tau$ , which implies that the noise causing the frequency instabilities has components at many frequencies. Therefore it is meaningless to specify fractional frequency deviation without a statement of averaging time.

The computing counter system is well-suited for this fractional frequency deviation measurement since it can make the frequency measurements  $f_i$  and  $f_{i-1}$  and immediately perform the data reduction necessary to solve Equation 1. It does all this automatically. The result  $\langle \sigma_{\Delta f/f}(2, T, \tau) \rangle$  is displayed on the computing counter after the  $N$  measurements and computations are performed.

An example of a fractional frequency deviation measurement performed by the computing counter system is illustrated in Fig. 4. A complete solution to Equation 1 is provided by the simple setup of Fig. 4(a). Either of the two programming devices, the 5375A Keyboard or the 5376A Programmer, can be used in this system. The keyboard program necessary to solve Equation 1 contains just 25 steps.<sup>6</sup>

Fig. 4(b) characterizes the oscillator noise in the time domain. Since the data reduction is performed by the measurement system in real time, it took only the time to make the frequency measurements to obtain the results shown. An additional benefit is the measurement resolution. The accuracy and resolution of the fractional frequency deviation measurement are directly related to the accuracy with which the individual frequency measurements can be made. The computing counter is the most accurate frequency

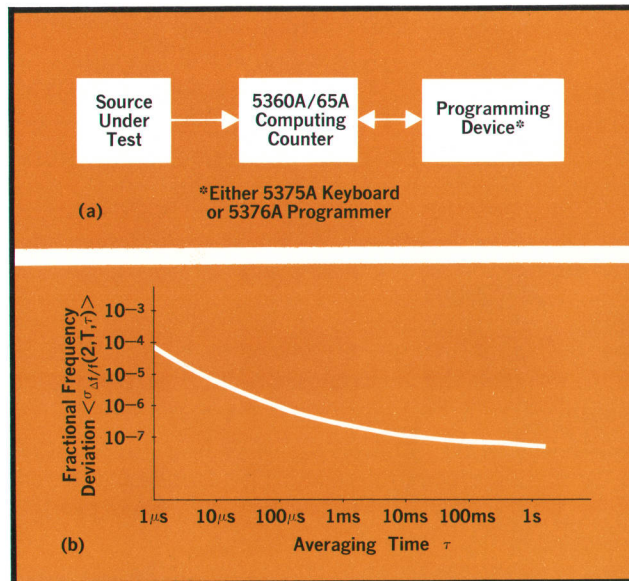


Fig. 4. Equipment setup and the results obtained in measuring fractional frequency deviation. Source under test was a 5 MHz oscillator.

counter in existence. Compared to a conventional frequency counter, the computing counter system is between 20 and 200 times more accurate in collecting the raw data. Also, the conventional counter has no data-reduction capability and the user must go off-line to a computer to obtain the final solution.

### Frequency-Domain Stability Measurements — Phase Noise

Related to phase noise is a fundamental frequency-domain stability parameter known as *spectral density*. The spectral density  $S_{\Delta f}(f_m)$  of an oscillator is a measure of the amount of noise power per unit bandwidth contributed by the random frequency fluctuations in the oscillator output at a frequency offset  $f_m$  from the nominal oscillator center frequency. Spectral density, a frequency-domain parameter, can be measured by the computing counter system, which makes measurements in the time domain, by means of the *Hadamard variance*  $\sigma_H^2$ . The Hadamard variance<sup>7</sup> is similar to the Fourier transform in that it transforms the raw time-domain data into meaningful frequency-domain data.

The relationship between spectral density  $S_{\Delta f}(f_m)$  and the Hadamard variance  $\sigma_H^2$  is given by

$$S_{\Delta f}(f_m) = \frac{N}{A_1^2 f_m} \sigma_H^2 - \left(\frac{A_3}{A_1}\right)^2 S_{\Delta f}(3f_m) - \left(\frac{A_5}{A_1}\right)^2 S_{\Delta f}(5f_m) - \dots \quad (2)$$

where  $A_j$  and  $N$  are constants (see Equations 3 and 5 below),  $S_{\Delta f}(jf_m)$  are spectral densities at frequency offsets  $jf_m$  from the nominal carrier, and  $j$  are odd positive integers. The Hadamard variance is in turn related to the frequency measurements of the oscillator under test by

$$\sigma_H^2(N, t, \tau) = \langle (f_1 - f_2 + f_3 \dots - f_{2N})^2 \rangle \quad (3)$$

where  $\tau$  is the averaging or measurement time of the individual frequency samples,  $t$  is the dead time between measurements,  $f_1, f_2, \dots$  are the data resulting from the individual frequency measurements over averaging time  $\tau$ , and  $N$  is the number of terms in the summation. The frequency offset  $f_m$  at which the spectral density is measured is selected by the times  $\tau, t$ , namely:

$$f_m = \frac{1}{2(\tau + t)} \quad (4)$$

The times  $\tau$  and  $t$  are adjustable over a wide range in the computing counter system, giving the system the ability to make measurements at any frequency offset  $f_m$  in the range  $0.01 \text{ Hz} \leq f_m \leq 150 \text{ Hz}$ . Thus spectral density measurements extremely close to the carrier can be made. On the other hand, the system is limited to a maximum offset of 150 Hz; however, the modern spectrum analyzer can comfortably handle offsets greater than this. The constants  $A_j$  of Equation 2 are also a function of  $\tau$  and  $t$ :

$$A_j = 2N \frac{\sin j\pi\tau/2(\tau + t)}{j\pi\tau/2(\tau + t)} \quad (5)$$

where  $j = 1, 3, 5 \dots$

Equations 2 and 5 indicate that on a broadband basis, the spectral density measurement includes information at odd harmonics as well as at the fundamental frequency  $f_m$  to which the system is tuned (Equation 4). Thus, as Fig. 5 illustrates, filtering should always be employed to remove unwanted noise components at frequencies outside the range of interest.

Equation 5 also indicates that  $A_j$  are functions of  $\tau$  and  $t$ , both of which are variables. This further helps in harmonic elimination since by selecting  $t = \tau/2$ ,  $A_3$  is reduced to zero, thereby eliminating the third harmonic from Equation 2.

The measurement procedure is to tune the system to the maximum offset  $f_{m \text{ max}}$ , and measure the spectral density  $S_{\Delta f}(f_{m \text{ max}})$ . This is repeated for other required offsets  $f_m < f_{m \text{ max}}$ , adjusting  $\tau$  and  $t$

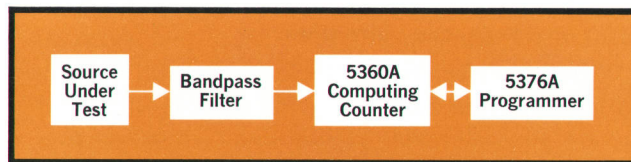


Fig. 5. Equipment setup for stability measurements in the frequency domain. Filtering is included here to remove noise components at frequencies beyond the range of interest.

so that  $t = \tau/2$ . Since the spectral density at other odd harmonics is now known, these can readily be eliminated. A typical result is shown in Fig. 6.

As noted earlier, the spectral density of frequency fluctuations  $S_{\Delta f}(f_m)$  is a fundamental frequency-domain stability parameter to which other parameters, some better known, are related. For example, the spectral density of phase fluctuations  $S_{\Delta\phi}(f_m)$  is related to  $S_{\Delta f}(f_m)$  by the equation

$$S_{\Delta\phi}(f_m) = \frac{1}{f_m^2} S_{\Delta f}(f_m) \quad \text{rad}^2/\text{Hz}. \quad (6)$$

Similarly, the single-sideband-to-carrier phase-noise power ratio is given by

$$\begin{aligned} \text{SSB/C Phase Noise} &= 10 \log \left( \frac{S_{\Delta\phi}(f_m)}{2} \right) \\ &= 10 \log \left( \frac{S_{\Delta f}(f_m)}{2f_m^2} \right) \end{aligned} \quad (7)$$

Using this equation, the data of Fig. 6 can be converted to these more familiar units, with the results shown in Fig. 7.

Either of Equations 6 and 7 can be solved and dis-

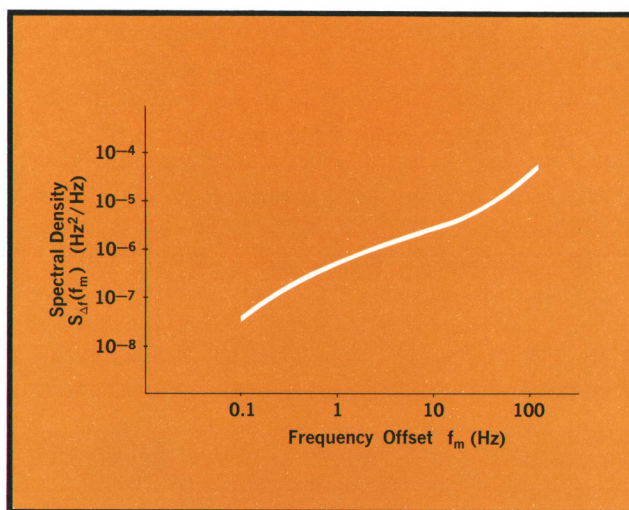


Fig. 6. Spectral density of 500 kHz voltage-controlled oscillator as measured by the setup of Fig. 5.

played automatically by the computing counter system with only minor differences in the program. The Hadamard variance is mathematically more complex than the Allan variance; hence the 5376A Programmer is the only 5360A programming device with sufficient capability to provide a total solution.

### Discrete Modulation Measurements — Frequency and Phase Deviation

The preceding section dealt with the frequency-domain measurement of random noise by means of the Hadamard variance. This same transform can be employed equally well to measure the rms frequency or phase deviation due to discrete modulation. For example, the rms frequency deviation  $\Delta f_{\text{rms}}$  is given by

$$\Delta f_{\text{rms}} = \frac{\sigma_H(N,t,\tau)}{A_1} \text{ Hz} \quad (8)$$

where  $\sigma_H(N,t,\tau)$  is given by Equation 3 and  $A_1$  is given by Equation 5.

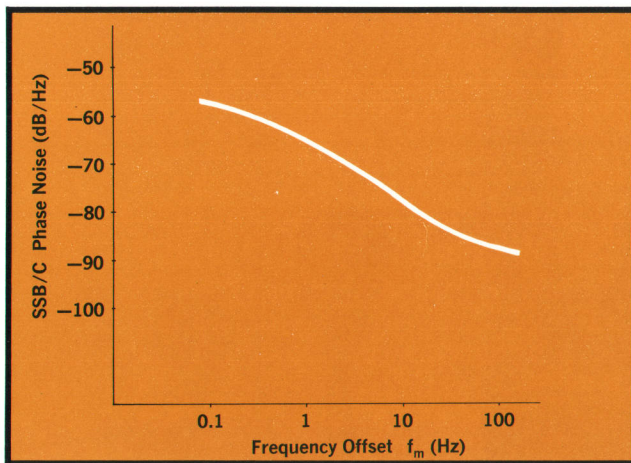


Fig. 7. Single-sideband-to-carrier phase noise of the oscillator represented in Fig. 6.

With an appropriate program in the 5376A Programmer, a total solution to Equation 8 can be obtained and displayed automatically by the computing counter system. The measurement procedure would be to tune the system to the frequency  $f_m$  at which the discrete modulation is occurring (see Equation 4), and with the equipment setup of Fig. 5 enter the program necessary to solve Equation 8. The measurement will be in error if appreciable noise or discrete modulation components are present at odd harmonics of the frequency  $f_m$  to which the system is tuned. However, the third harmonic can be eliminated by

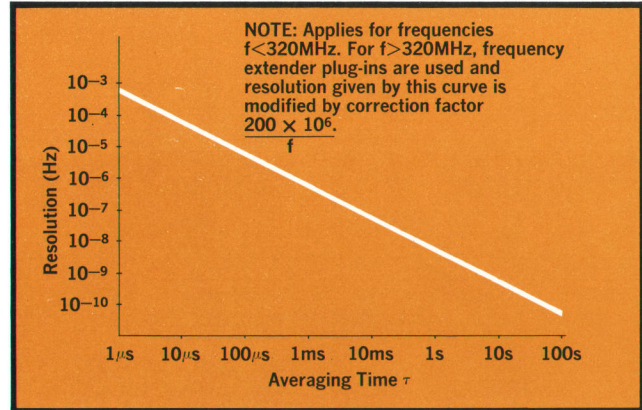


Fig. 8. Resolution of fractional frequency deviation measurements with the 5360A System.

setting  $t = \tau/2$  and other harmonics can be removed by filtering, if necessary.

In a similar manner the rms phase deviation  $\Delta \phi_{\text{rms}}$  due to discrete phase modulation can also be measured. This parameter is given by

$$\Delta \phi_{\text{rms}} = \frac{\Delta f_{\text{rms}}}{f_m} = \frac{\sigma_H(N,t,\tau)}{f_m A_1} \text{ rad.} \quad (9)$$

A simple extension of this procedure gives a measurement of intermodulation distortion. The measurement procedure is to apply two frequency modulation signals at  $f_1$  and  $f_2$  and tune the system to  $(f_2 - f_1)$ . The presence of a discrete component at  $(f_2 - f_1)$  indicates the device under test has finite intermodulation distortion.

### Resolution and Dynamic Range of Stability Measurements With the Computing Counter System

A glance at Equation 1 shows that the greater the frequency measurement accuracy the better the resolution of the fractional frequency deviation measurement. The computing counter is the most accurate direct-frequency-measuring device available. It is so accurate, in fact, that the computing counter system can measure fractional frequency deviations as small as  $5 \times 10^{-10}$  for 1 second averaging times.

The resolution of fractional frequency deviation measurements with the computing counter system is shown in Fig. 8 as a function of averaging time. The resolution is sufficient to measure the stability of most frequency sources except high-performance crystal oscillators and atomic frequency standards. Even these can be measured by an indirect technique. The measurement setup requires more equipment than is shown in Fig. 4(a), but the procedure is

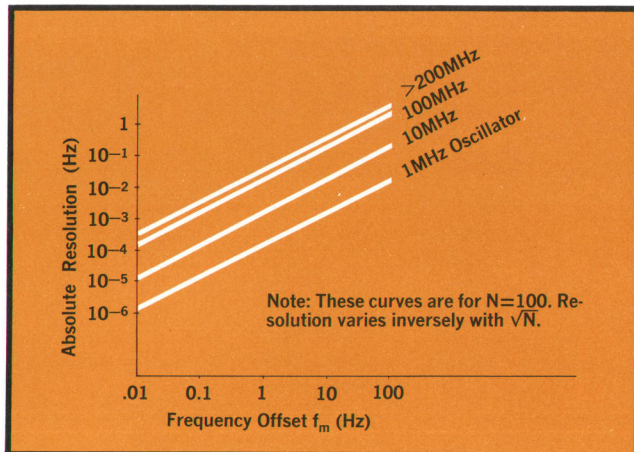


Fig. 9. Resolution of Hadamard variance measurements with the 5360A System.

identical. The indirect measurement technique is fully described in reference 8.

Fig. 9 defines the resolution of the computing counter system in the Hadamard variance measurement. Again, its resolution is sufficient for most sources except high-performance crystal oscillators and atomic standards. The indirect measurement technique is also applicable to these frequency-domain stability measurements.

The Hadamard variance is the basis for all frequency-domain stability measurements with the computing counter system. The dynamic range of the system in any frequency-domain measurement can be determined using Fig. 9 and Equations 2 through 7.

#### Acknowledgment

I am grateful to Dick Baugh, who did the original work relating the Hadamard variance to frequency stability and gave invaluable advice and assistance in the preparation of this article. 🍷

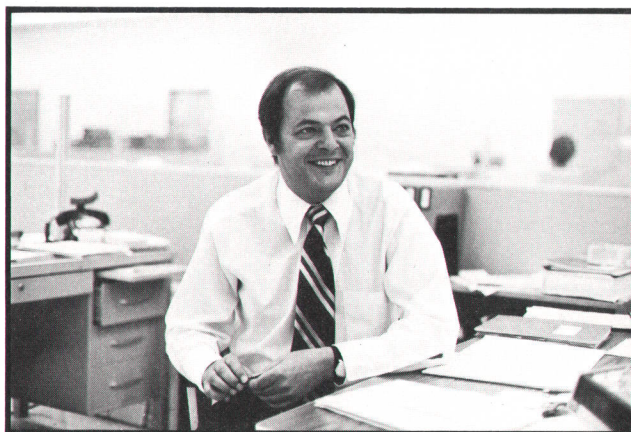
#### References

1. G. B. Gordon and G. A. Reeser, 'Introducing the Computing Counter,' **Hewlett-Packard Journal**, May 1969.
2. K. M. Ferguson, 'The Computing Counter Gets Its Keyboard,' **Hewlett-Packard Journal**, March 1970.
3. D. Martin, 'Computing-Counter Measurement Systems,' and E. M. Ingman, 'Programmer Is Key to Computing-Counter Systems,' **Hewlett-Packard Journal**, December 1970.
4. D. W. Allan, 'Statistics of Atomic Frequency Standards,' *IEEE Proceedings*, Vol. 54, No. 2, 1966.
5. NBS Technical Note 394, 'Characterization of Frequency Stability.'
6. Hewlett-Packard Computing Counter Applications Library No. 7, 'Fractional Frequency Deviation of

Oscillators.'

7. R. A. Baugh, 'Frequency Modulation Analysis with the Hadamard Variance,' *Frequency Control Symposium*, April 1971.

8. Hewlett-Packard Application Note 116, 'Precision Frequency Measurements.'



#### David Martin

Dave Martin is product marketing manager for counters and printers at HP's Santa Clara Division. A native of Australia, Dave holds two baccalaureate degrees from the University of Sydney, one in physics and mathematics (1961) and the other in communications engineering (1963). He first joined HP in Australia in 1966, then came to the U.S. in 1967 to join the factory computing-counter marketing team. He later became product manager for the computing counter system and then product manager for high frequency counters. He assumed his present job this year. This article is his second contribution to the *Hewlett-Packard Journal*.

# More Informative Impedance Measurements, Swept from 0.5 to 110 MHz

*An accessory Probe converts the Model 8407A Network Analyzer into a vector impedance measuring system that gives instantaneous swept display of a component's or network's complex impedance versus frequency. The system compensates for the effects of the Probe's own capacitance and inductance on the measurement.*

By Julius K. Botka

IMPEDANCE, a concept fundamental to circuit design, is progressively more difficult to measure as test frequencies go much above the audio range. Factors such as lead inductance, parasitic capacitance, and core losses very often cause a component's high-frequency impedance to be quite different from that expected. For high-frequency circuit design and analysis, then, it is important to be able to measure component impedance.

Because the simple act of connecting a measuring instrument to a component adds reactance, impedance measurements are not as straightforward at higher frequencies as one would wish. Although there are instruments such as Q meters and RX meters that obtain accuracy at high frequencies, one would hope for the same kind of speed, convenience, and detail in impedance measurement that one has become accustomed to with swept-frequency network analyzers.

The Hewlett-Packard Model 8407A Network Analyzer brought this ideal a step closer to reality. Because this instrument measures ratios, it can measure impedance with a voltage probe on the TEST input and a current probe on the REFERENCE input. But, as would be expected, the parasitic inductance and capacitance introduced by previously available probes usually limits these measurements to the lower RF frequencies (e.g. <10 MHz).

Consequently, a new accessory probe for the 8407A Network Analyzer has been developed (Fig. 1). The objective here was to make a ratio measurement possible with only one probe, and to accommodate probe reactances in a practical manner. As a result, the Probe design reduces the effect of parasitic inductance on the display essen-

tially to zero, and inductance added by adapters or other connectors can be accounted for easily. The effect of Probe and adapter parasitic capacitance is canceled out by an adjustable circuit.

Because of its near-zero effective reactance, the new Probe (Hewlett-Packard Model 11655A) makes possible swept-frequency measurements of impedance magnitude and phase with typically 5% accuracy within a frequency range of 5 to 110 MHz, and down to 0.5 MHz with decreasing accuracy. Fixed frequency measurements can be made down to 100 kHz with better than 5% accuracy. The display is quickly calibrated with a built-in 100 $\Omega$  standard and measurements can then be made with touch-and-read convenience and without need for any other zeroing or balancing adjustments.

The range of impedance measured is considerable: from 0.1 $\Omega$  to greater than 10k $\Omega$ , a range of 10<sup>5</sup>:1. The instrument can display as much as 10<sup>4</sup>:1, 1 to 10k $\Omega$ , all at one time, a dynamic range that is especially useful when resonant peaks and dips are encountered (Fig. 2). Measurements of 0.1 $\Omega$ , next to impossible at 100 MHz by any previous techniques, are easily performed.

Measurement results may be displayed in one of two ways. With the Analyzer's Magnitude-Phase Display plug-in (Model 8412A) the system presents two traces on its CRT display, one representing the absolute magnitude of impedance versus frequency and the other representing phase angle. With the Analyzer's Polar Display plug-in (Model 8414A), impedance is presented on Cartesian coordinates as  $R \pm jX$  (Fig. 3). Either display tells the complete story, with no information-hiding gaps in frequency coverage.

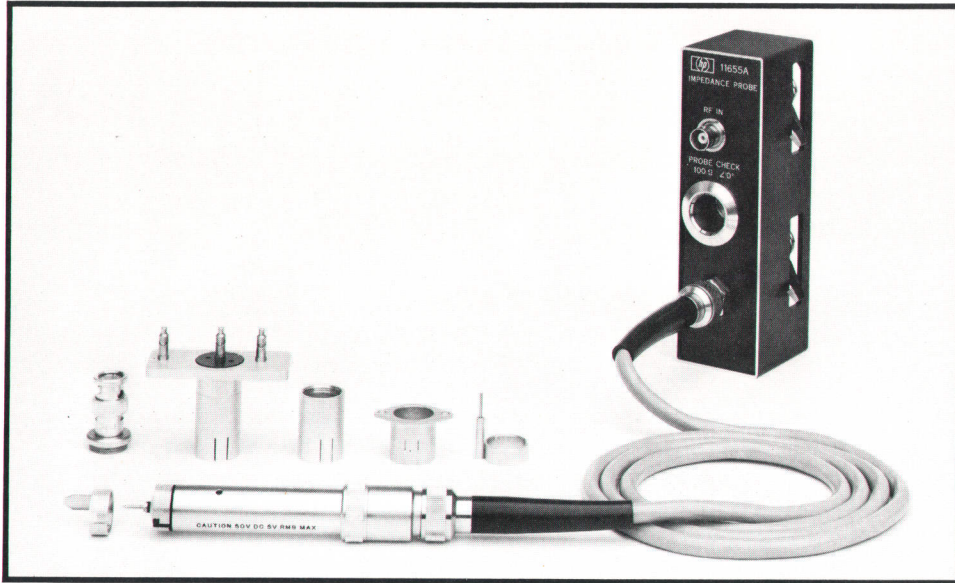


**Fig. 1.** Model 11655A Impedance Probe is supplied with variety of adapters to meet common measurement situations.

### A Range of Applications

The uses for the new impedance measuring system are manifold. Circuit designers can quickly determine the characteristics of components, thereby reducing the amount of cut-and-try needed to achieve desired circuit performance. It is particularly handy for measuring the characteristics of highly reactive devices, such as recording heads. Because the system presents impedance information graphically over the frequency range of interest, it becomes easy to trim impedances—adjusting the lead length of capacitors, for example, to place the capacitor self-resonance where it won't hurt circuit performance.

In production tests, the new system can determine the acceptability of circuits by measuring

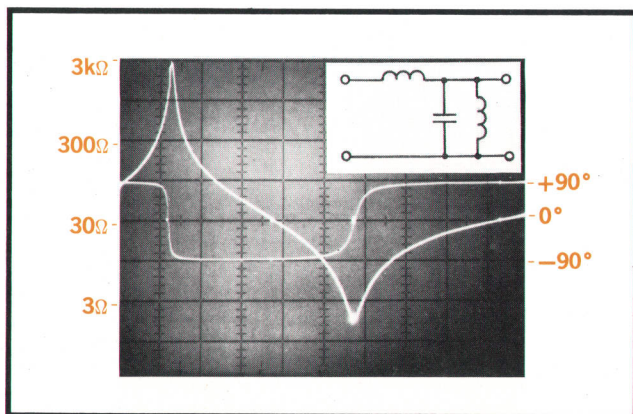


**Fig. 2.** Swept display of circuit impedance clearly shows frequencies of parallel and series resonances. Impedance phase angle is shown by trace that switches between +90° and -90° levels.

the impedance throughout the circuit's operational frequency range at selected terminals. It can do things like check the characteristic impedances of long coaxial cables without requiring termination of the far end of the cable (Fig. 4).

The Probe/Analyzer system can also measure the impedance of active circuits everywhere in the selected frequency range except at frequencies where the circuit itself may generate an output. This application of the Probe, and also its use in measuring negative impedances, will be discussed later in this article.

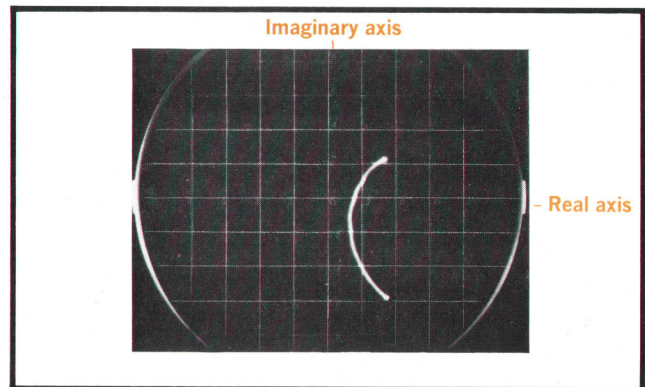


**Fig. 3.** Impedance of folded dipole antenna over 88-108 MHz frequency range as displayed on Cartesian coordinates with Model 8414A Polar Display. Full scale is 1000Ω. At 88MHz (lower bound of trace) antenna impedance reads as 350-j600Ω.

### What's Inside

Essentially, the Probe measures the voltage across and the current flowing into the unknown.

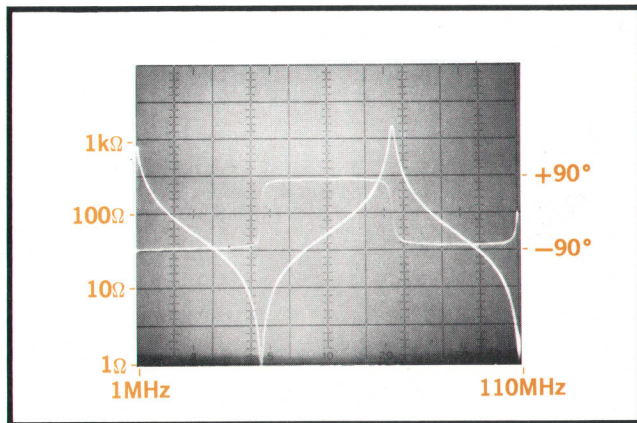


Fig. 4. Impedance display shows electrical length of unterminated, (open-circuited) 50Ω cable to be  $\frac{3}{4}\lambda$  at 110MHz. Phase of impedance jumps from  $-90^\circ$  (capacitive) to  $+90^\circ$  (inductive) every  $\frac{1}{4}\lambda$ . Line's characteristic impedance is found at odd multiples of  $\frac{1}{8}\lambda$ , shown here to be 50Ω (6dB below 100Ω). This technique can disclose characteristic impedance and electrical length of unknown cable wound on spool.

The ratio, determined by the Network Analyzer, gives the absolute magnitude of the impedance  $|Z|$ , and the Analyzer's measurement of the phase angle between voltage and current waveforms gives the phase angle  $\theta$  of the impedance.

Measurement stimulus is supplied by a suitable sweep-frequency generator, such as the Hewlett-Packard Model 8601A (Fig. 5). As shown in Fig. 6, RF voltage from the sweep generator is fed into transformer T1. The voltage appearing across output winding N2 is applied to the probe terminals. This voltage is sensed by transformer T3 and the result is applied to the TEST input of the Network Analyzer. No attempt is made to maintain the probe terminal voltage constant since all that is desired is the ratio of voltage to current.

Current flowing through the unknown contacted by the Probe is sensed by transformer T2. The output of T2 is applied to the REFERENCE input of the Network Analyzer.

Current flowing in the parasitic capacitance in the Probe, and in a component-holding fixture that may be used, is canceled by an out-of-phase current taken from winding N3 of input transformer T1. The phase of this current is adjusted by the delay line (a section of high impedance line) and by the relative inductance of windings N2 and N3 of T1. The magnitude of current is externally adjusted by capacitor C1.

The adjustment for proper cancelation is easily made. The Probe is detached from the device to be measured and, with the component adapter in

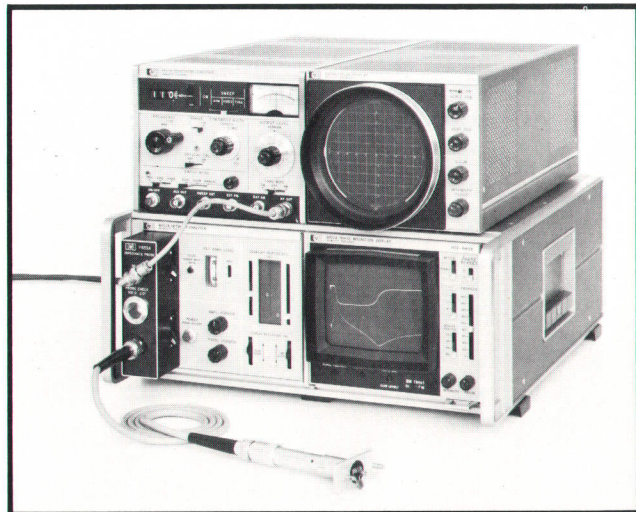


Fig. 5. Complete impedance measuring system includes Probe, Network Analyzer with either or both display plug-ins, and RF Generator/Sweeper.

place (if used), C1 is adjusted to arrive at a display that shows zero capacitive reactance.

Unwanted voltage resulting from parasitic inductance is canceled by coupler T4 between the current-sensing and voltage-sensing transformers. This coupler is adjusted during production test to achieve zero inductive reactance on the display with the socket of the removable probe tip shorted to the middle of the grounding ring. The inductive reactance added by a component adapter is then easily measured by shorting the point of measurement with a brass plate and noting the resulting reading. This can be subtracted from subsequent measurements to get the true value of impedance in the external circuit.

When properly adjusted to cancel parasitic reactance, and with parasitic inductance in the measurement set-up (if adapter is used) discounted for, the Probe's residual parasitics, as far as the measurement is concerned, are purely resistive, as shown in Fig. 7. The values of  $R_p$  and  $R_s$  can be used to calculate the true values of impedance when measuring at either the low or high end of the Probe's impedance range.

#### Measurements in Active Circuits

As mentioned previously, the Probe can measure impedances of active circuits while the circuit is in operation. Since the 8407A Network Analyzer functions as a selective detector, it discriminates against any outputs generated by the circuit itself. Care must be taken, though, to ensure that the probe is not overloaded.

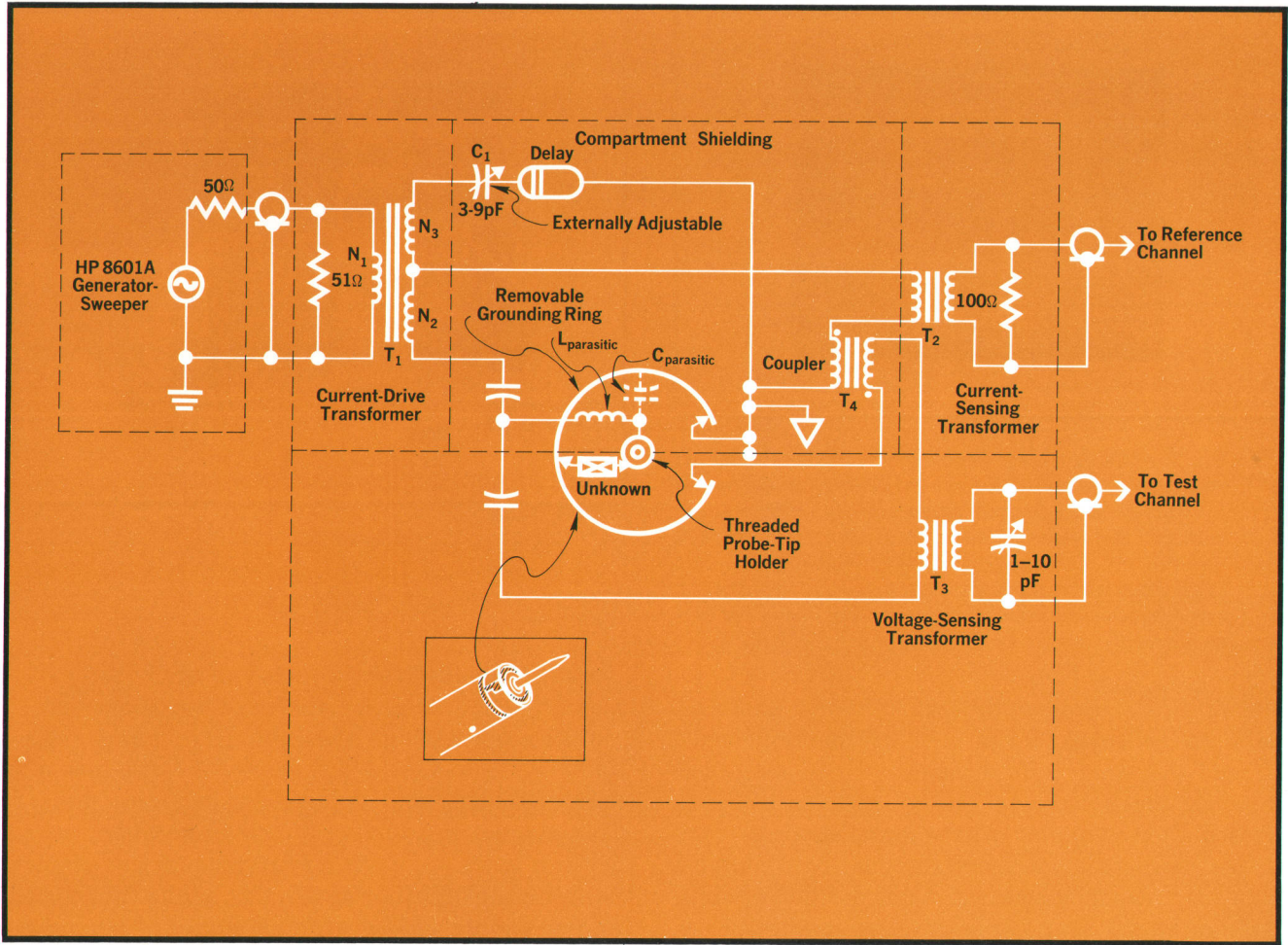


**Fig. 6.** Probe circuit. Grounding ring is gapped so that current in T2 circuit does not flow on T3 side of shielding and vice versa. For this reason, to achieve minimum effective parasitic inductance, unknown circuit ground should contact grounding ring at point opposite to gap.

To prevent overload of active circuits, the Probe drive signal should be reduced from the normal  $-3\text{dBm}$  to  $-18\text{dBm}$ , which reduces the drive at the probe tip from  $135\text{ mV}$  to  $24\text{ mV}$ . This reduces the dynamic range, of course, but the minimum measurable impedance is still  $1\Omega$ .

The operator should be aware, however, that although the equivalent impedance that the Probe presents to the unknown does not affect the measurement itself, it could shift the resonant frequency of an oscillator circuit.

The Probe can also measure negative imped-

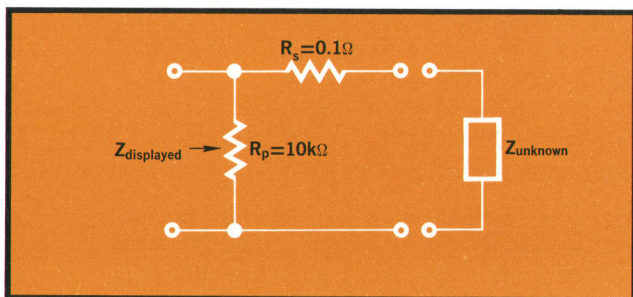


**Fig. 7.** Equivalent circuit of Probe is purely resistive when Probe's parasitic reactances are balanced out.

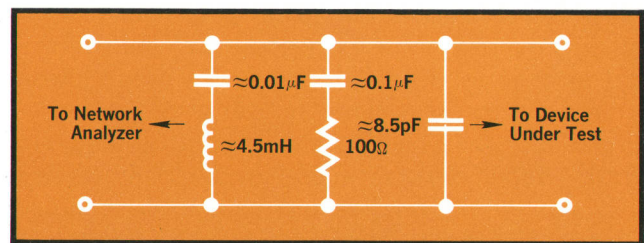


**Fig. 8.** Effect of Probe's passive impedance on active network should be considered when measuring active circuit. Probe's impedance, diagrammed here, does not affect measured values, however.

ances, such as that of a tunnel-diode shown in Fig. 9. In this case, the tunnel diode was biased into the negative impedance region through an inductor large enough to prevent the bias supply from shunting the diode impedance, but low enough in resistance to avoid parasitic oscillations.

#### Acknowledgments

John Marshall contributed to the mechanical design of the new Probe. Many helpful suggestions were provided by Stephen Adam, Philip Spohn, Richard Hackborn, David Gildea and Earl Heldt. ☺

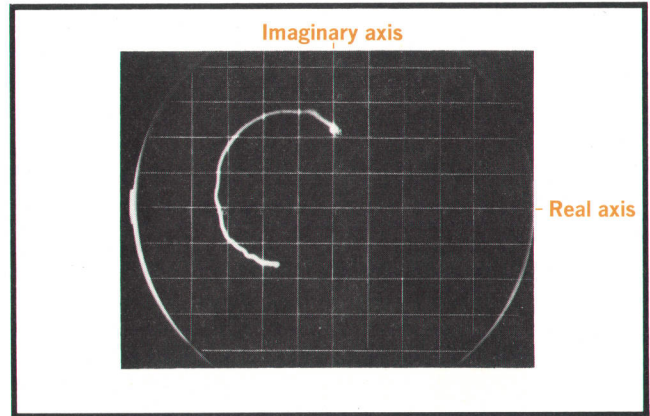


Fig. 9. Display of negative impedance of tunnel diode.

### SPECIFICATIONS HP Model 11655A

#### Impedance Probe (with 8407A Network Analyzer)

##### FREQUENCY RANGE:

0.5 MHz to 110 MHz (measurements to 100 kHz are possible).

##### IMPEDANCE MEASUREMENT RANGE:

AMPLITUDE: 0.1Ω to >10 kΩ.

PHASE: 0° ±90°.

##### ACCURACY\*:

##### SINGLE FREQUENCY MEASUREMENT (0.5 MHz to 110 MHz):

Amplitude: ±5% or +0.035Ω, -0.07Ω, whichever is greater.

Phase: ±5° for |Z| >3.16Ω, decreasing to ±25° at 0.1Ω.

Note: Measurements can be made from 0.1 MHz to 0.5 MHz with accuracy decreasing to typically ±10% in amplitude and ±10° in phase at 0.1 MHz for impedance magnitudes between 0.1Ω and 1 kΩ.

##### SWEPT FREQUENCY MEASUREMENT:

Amplitude: Typically ±5% between 3 and 110 MHz, decreasing below 3 MHz to typically ±30% at 0.5 MHz.

Phase: Typically ±5° between 5 and 110 MHz for |Z| >3.16Ω, decreasing below 3.16Ω to ±25° at 0.1Ω.

##### INTERNAL CALIBRATOR:

Amplitude: 100Ω ±0.5%.

Phase: 0° ±2°.

##### SIGNAL LEVELS APPLIED TO DEVICE UNDER TEST FROM IMPEDANCE PROBE:

135 mV rms for Sweep Oscillator output of -3 dBm (typical level for passive devices).

24 mV rms for Sweep Oscillator output of -18 dBm (typical level for active devices).

##### RESOLUTION:

8412A Phase-Magnitude Display (0.1 kHz BW):

1% magnitude and 1° phase for |Z| >3.16Ω.

8414A Polar Display:

5% magnitude and 2° phase for |Z| >10Ω.

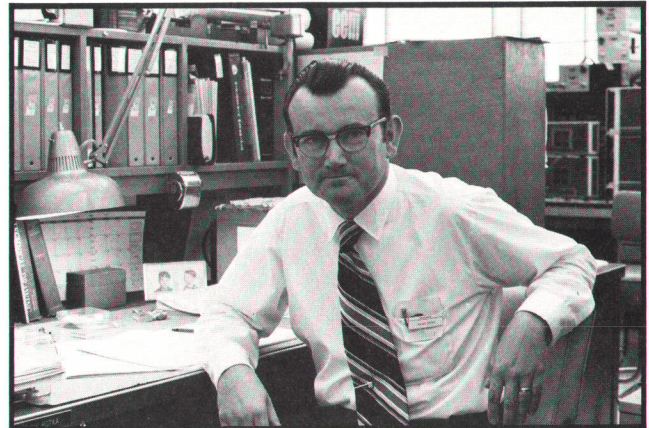
##### MAXIMUM EXTERNAL VOLTAGE TO PROBE: 50 V dc, 5 V rms.

##### CABLE LENGTH: 48 inches.

##### PRICE: \$750.00

\* Accuracy specifications include total system (probe, analyzer, calibrator) and are valid if input power to Probe is -3 dBm, system is calibrated with 100Ω calibrator, capacitive Probe parasitics are balanced out, and effect of Probe's resistive residuals on measurement display are considered (see text).

MANUFACTURING DIVISION: MICROWAVE DIVISION  
1501 Page Mill Road  
Palo Alto, California 94304



#### Julius K. Botka

Julius Botka has been with HP six years, first evaluating microwave solid-state devices as part of the HP Associates applications group, then developing mixers in the R and D lab, and finally as a development engineer working on Network Analyzer accessories in HP's Microwave Division engineering lab.

Julius received his education at the Technical Institute, Budapest, Hungary. He came to the United States in 1957 and operated his own communications equipment service business in Miami, Florida. He moved to California five years later and, before joining HP, worked on the development of A-D converters, high-speed multiplexers, solid-state switching circuits, and automatic frequency control for radars. When he finds time, he enjoys tennis, sailing, and amateur astronomy.

U. S. Naval Observatory  
Washington, D. C. 20390

Time Service Announcement, Series 14

No. 8 (abbreviated)

8 October 1971

## New UTC System

### References:

- (a) Time Service Announcement Series 14, No. 7
- (b) CCIR Rec. VII/460 (New Delhi, 1970)
- (c) IAU Rec. 1 of Comm 31 (Brighton, 1970)
- (d) CCIR Report VII/517 (Geneva, 1971)
- (e) "International Coordinated Clock Time and the Coming Improvements in the System UTC," by G. M. R. Winkler, *25th Annual Frequency Control Symposium*, Atlantic City, N. J., April 1971
- (f) Time Service Announcement Series 14, No. 2

1. In accordance with References (b), (c), and (d), the following improvements in the system of coordinated clock time used by USNO for all external measurements will be implemented on 31 December 1971 at 24 hours UTC.

a) Frequency Change:  
The frequency of UTC (USNO) will be increased by  $300 \times 10^{-10}$ . This is equivalent to permanently making the "Offset" zero. (Clocks will operate on standard frequency as based on the S.I. second.)

b) Time Step:  
At the end of this calendar year a unique fraction of a second step will also be introduced in UTC (USNO) to coordinate it closely with the International Time Scales kept by the BIH. UTC (USNO) will be delayed (retarded) by 107 600  $\mu$ s. In other words, the standard moment of change may be expressed in either of the following dates which will mean the same instant.  
1971 December 31, 23<sup>h</sup> 59<sup>m</sup> 60<sup>s</sup>.107 600 old UTC.  
1972 January 1, 0<sup>h</sup> 0<sup>m</sup> 00<sup>s</sup> (exactly) new UTC.

2. Difference: UTC (USNO, new) - UTC (USNO, old)  
The difference for the instant of measurement may be computed directly from the following formula by converting the desired instant to a decimal of a day.

$$\text{UTC (USNO, new)} - \text{UTC (USNO, old)} = 2\,592 (\text{MJD} - 41317) - 107\,600 \mu\text{s}.$$

### Example:

Time of measurement:  
1971 October 15, 8<sup>h</sup> 15<sup>m</sup> 26<sup>s</sup> UTC (old or new) = MJD  
41239.344 051

The formula gives  
 $\text{UTC (USNO, new)} - \text{UTC (USNO, old)} =$   
 $-308884.22 \mu\text{s}.$

3. Further details of the coming changes in the coordinated clock time system can be found in References (a) and (e). Details concerning the Delta UT Code (giving  $\Delta\text{UT} = \text{UT1} - \text{UTC}$ ) can be found in References (d) and (e). (Reference (a) is superseded by Reference (d) in regard to the code.)

4. In view of the coming improvements, no further steps will be announced in the old UTC. Consequently, users requiring UT1 or UT2 with greater precision than 0.7s are advised to request Time Service Announcement Series No. 7, issued weekly. It gives predicted differences for UT2 - UTC two weeks in advance with an estimated accuracy of 5 ms.

Gernot M. R. Winkler  
Director  
Time Service Division

Bureau International De L'Heure  
61, Avenue de l'Observatoire  
75 — PARIS 14ème

## Time Step and Elimination of the Frequency Offset of the UTC System

According to the CCIR Recommendation 460 (New-Dehli, 1970), to the IAU Recommendation 1 of Commission 31 (Brighton, 1970) and to the CCIR Report 517 (Genève, 1971), notice is hereby given that:

1. On the 1st of January 1972, a negative time step of  $-0.1077577$  s will be applied to UTC, under the following conditions: The time step will occur when the date will be:

1971, Dec. 31, 23h 59m 60<sup>s</sup>.1077577, old UTC, so that at this instant the date will become 1972, Jan. 1, 0h 0m 0s (exactly), new UTC.

2. The frequency offset of the presently used UTC ( $-300 \times 10^{-10}$ ) will be eliminated at the instant of the above time step.

B. Guinot  
Director

### Comments and Notes

a. Dating the events in the vicinity of the time step and frequency step. The rules of Annex I to CCIR Report 517 apply.

b. Second order terms of the frequency offset were taken into account by assuming that in the relationship

$$\text{AT(BIH)} - \text{UTC} = 4.213170\text{s} + (\text{J.D.} - 2439126.5) \times 0.002592 \text{ s d}^{-1}$$

the julian day number is computed in atomic days since 1958, January 1st, when the atomic time was approximately in coincidence with UT. When J.D. is expressed in universal time days, the difference amounts to 0.3  $\mu$ s.

c. The approximation of UTC kept by the laboratories and designated by UTC(i) (CCIR recommendation 457 New-Dehli, 1970) might be put in agreement with UTC by the extrapolation of UTC-UTC(i) published in the BIH Circular D.

d. The value of DUT1 to be used from the 1st of January 1972 will be sent in due time to the organizations listed on pages 78 and 79 of the BIH Annual Report for 1970.

e. The date of occurrence of a leap second will be given 8 weeks in advance to the same organizations as in (d) and, in addition, to some international organizations (IAU, ICSU, CCIR, CIPM, UGGI, UIT, URSI), to the National adhering Organizations and National Correspondents to ICSU.

Editor's note: It is to be expected that each national time service will make a somewhat different time announcement. This is because differences of as much as a millisecond exist among them. These differences will be smaller after January 1, 1972.